

## Source Parameters of Some Large Earthquakes in Northern Aegean Determined by Body Waveform Inversion

ANASTASIA A. KIRATZI,<sup>1</sup> GREGORY S. WAGNER<sup>2</sup> and CHARLES A. LANGSTON<sup>2</sup>

*Abstract*—Average source parameters for three large North Aegean events are obtained from body wave inversion for the moment tensor. The parameters for the events are as follows:

Date	$M_s$	$M_0 \cdot 10^{25}$ dyn-cm	Strike°	Dip°	Rake°	Depth
Feb. 19, 1969	7.1	22.4	216	81	173	10 km
Dec. 19, 1981	7.2	22.4	47	77	-167	6 km
Aug. 6, 1983	6.8	12.1	50	76	177	9 km

The events exhibit dextral strike-slip faulting with the  $T$  axis striking NS and nearly horizontal, implying extension in this direction. The focal mechanisms obtained are in agreement with the seismotectonic regime of the North Aegean. It is known that the region is tectonically controlled by the existence of the strike-slip Anatolian fault and its westward continuation in the Aegean, as well as the NS extension the whole Aegean area undergoes.

The components of the moment tensor show that the region is dominated by compression in the EW direction which is encompassed by extension in the NS direction. All the events were found to be shallow ( $\leq 10$  km) with a source time function of approximately 8 s duration and small stress drop values.

The teleseismic long period vertical  $P$ -waves exhibited distortions, that could be attributed to lateral inhomogeneities in the source structure or more probably to a nonflat water-crust interface.

**Key words:** Moment tensor inversion, North Aegean, Greece.

### 1. Introduction

The Aegean and surrounding region is an area of intense seismic activity. Focal mechanisms and Neogene-Quaternary geology indicate a very complex and rapidly varying tectonic picture.

The northernmost part of the Aegean area, the North Aegean trough, 1000–1500 m deep, is more than 500 km from the lithospheric boundary of the Hellenic

<sup>1</sup> Geophysical Laboratory, University of Thessaloniki, 540 06, Greece.

<sup>2</sup> Department of Geosciences, 403 Deike Building, Pennsylvania State University, University Park, PA 16802, U.S.A.

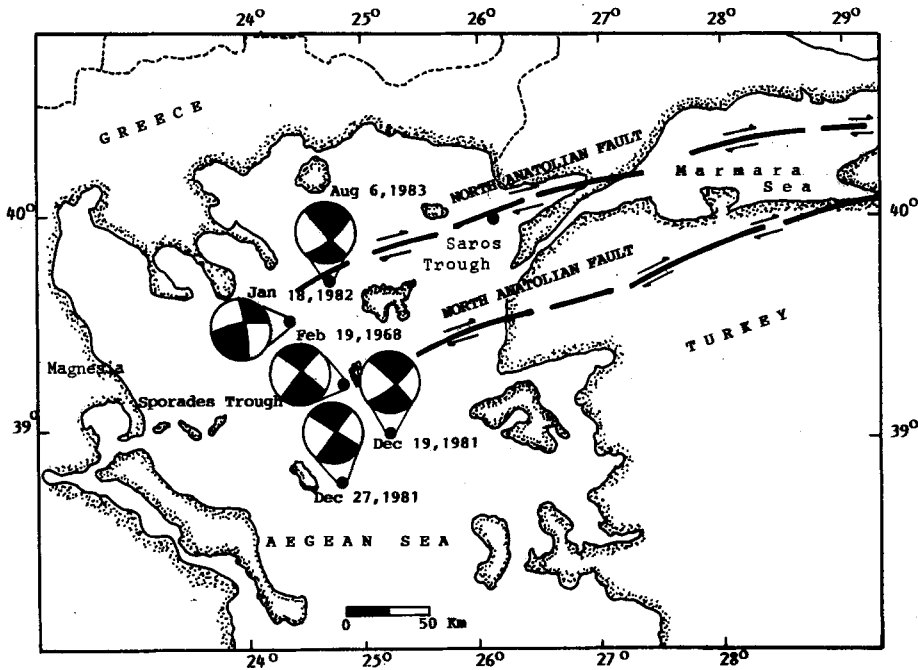


Figure 1

The North Aegean trough system with lower hemisphere projections of fault mechanisms determined in this study together with those of December 27, 1981 (KING and KIRATZI, 1985) and of January 18, 1982 (PAPAZACHOS *et al.*, 1984).

arc. This graben which extends from the Saros trough to the east as far as Magnesia to the west (Figure 1), takes up the dextral strike-slip motion of the North Anatolian fault at its western termination. The North Anatolian fault, which began in the middle to late Miocene time to absorb the relative motion between the Anatolian and Black Sea plates, consists mainly of two active strands, both which continue in the Aegean (PAPAZACHOS *et al.*, 1986).

The trough itself and the surrounding basins constitute the southern margin of the European plate which is less deformed than the Hellenic arc (MCKENZIE, 1972, 1978; LEPICHON and ANGELIER, 1979).

The area has suffered numerous earthquakes, the most recent started in December, 1981 with a series of strong events which ended in November, 1983. In this paper, moment tensor inversion analysis is performed for the following events: February 19, 1968 with  $M_s = 7.1$  and epicenter  $39.4^\circ\text{N}$ ,  $24.9^\circ\text{E}$ ; December 19, 1981 with  $M_s = 7.2$  and epicenter  $39.1^\circ\text{N}$ ,  $25.2^\circ\text{E}$ ; and August 6, 1983 with  $M_s = 6.8$  and epicenter  $40.1^\circ\text{N}$ ,  $24.8^\circ\text{E}$ . Focal mechanisms based on first motion data have already been published for these events by MCKENZIE (1972), PAPAZACHOS *et al.* (1984), and ROCCA *et al.* (1985). The need for reliable fault plane solutions, so as to understand the complicated tectonics of this area, motivated the present paper.

Moreover, the region is very important relative to seismic hazard since new activity is expected to burst there soon (KARACOSTAS *et al.*, 1986).

## 2. Theory and Data Processing

The moment tensor formalism of the seismic source inverse problem has received considerable attention due to its obvious simplicity and linearity (LANGSTON, 1981). The feasibility of the method is based upon the fact that an arbitrarily oriented point shear dislocation (i.e., having a body force equivalent to the double couple) can be represented by the summation of three Green's functions (LANGSTON and HELMBERGER, 1975). LANGSTON (1981) derived expressions to linearize the displacement equations, using the moment tensor formalism. Briefly, the inversion involves determining the parameter change matrix ( $\Delta P$ ) in the matrix equation  $A \Delta P = \Delta c$ .  $A$  is the matrix of partial derivatives of the synthetics with respect to each parameter. The  $\Delta c$  matrix is the difference between the synthetic seismograms, (computed using some starting parameters) and the observed data. The  $A$  matrix is computed analytically using the equations for the synthetic seismograms and the Green's functions calculated for an assumed focal depth and source structure. Singular value decomposition is used to determine the inverse of the  $A$  matrix. For more details of the method refer to LANGSTON (1981), BARKER and LANGSTON (1982) and PAVLIN and LANGSTON (1983).

For the present work, microfiche records of both long- and short-period seismograms for the events studied were obtained from the WWSSN archives. Records were principally selected for inversion from stations in the range of  $30^\circ$  to  $90^\circ$  to avoid complexities in the waveforms caused by upper mantle and core-mantle boundary structures.

Table 1 lists the stations, from which the records were used in the inversion for each earthquake separately. As shown, the azimuthal coverage is sufficient in all cases. The long-period seismograms were digitized twice (top and bottom of the trace line) for better accuracy. The  $S$ -wave data were rotated into the respective station's back azimuth in order to extract long-period  $SH$ - and  $SV$ -waveforms. The use of  $P$ -,  $SV$ , and  $SH$ -waves, with their different radiation patterns allows the moment tensor elements to be better resolved. Moreover, effects of unmodelled structure near the source and along the ray path are decreased by inverting the  $P$ - and  $SH$ -,  $SV$ -seismograms from all stations simultaneously.

Green's functions for a point source with a step dislocation in a plane-layered medium were computed for different source depths, employing the ray theory technique outlined in LANGSTON and HELMBERGER (1975). The source region velocity structure listed in Table 2 was used (PANAGIOTOPOULOS and PAPA-ZACHOS, 1985) and the Green's functions were determined by summing rays for vertical strike-slip, vertical dip-slip and  $45^\circ$  dip-slip sources embedded at various

Table 1  
*WWSSN body wave data included in the inversions*

Station	$\Delta^\circ$	$Az^\circ$	$Baz^\circ$	$P$	$SH$	$SV$
<i>Event of February 19, 1968</i>						
AAE	33	154	340	+		
ATL	82	307	47	+	+	
BEC	70	296	55	+	+	
BLA	77	308	50	+		
BUL	60	176	357	+		
COL	76	357	6	+		
GDH	50	332	84	+	+	
KOD	55	107	311	+		
NAI	42	162	346	+		
OGD	71	308	54	+		
PRE	65	177	357	+		
QUE	35	92	297	+		
TRN	80	276	51	+		
WES	69	308	56			
<i>Event of December 19, 1981</i>						
BLA	78	308	50	+		
CAR	85	279	51	+		
COL	76	357	6	+	+	+
GDH	50	333	84		+	
KEV	31	1	183	+		
NDI	44	88	298	+		
PDA	39	284	72	+		
POO	47	102	307	+		
SHL	57	83	302	+		
WES	69	308	56	+		
<i>Event of August 6, 1983</i>						
AAM	75	313	49		+	
AKU	35	311	115	+		
ANP	79	67	309		+	+
BLA	77	308	49	+		
BUL	60	176	357	+		
COL	75	357	6	+	+	+
DAG	41	346	127		+	
KOD	55	108	312	+		
MAT	82	48	315	+		
NAI	43	162	346	+		
NDI	44	88	299	+		
SNG	75	94	310	+		
TRN	80	276	51	+	+	+
WES	68	307	55	+		

Table 2

*Crustal structure model at the source used in calculating synthetic seismograms*

$V_p$ (km/sec)	$V_s$ (km/sec)	Density (gr/cm <sup>3</sup> )	Thickness (km)
1.50	0.001	1.00	1.0
6.30	3.50	2.70	30.0
7.90	4.39	3.35	Half-space

depths in the particular velocity structure assumed. Receiver structures are assumed to be a homogeneous half-space. Responses from 33  $P$ - and 3  $SH$ -,  $SV$ -rays, which included all significant arrivals within the first 35 s of the signal for  $P$  and  $SV$ -waves and 25 s for  $SH$ -waves, were calculated and, summed up. These responses were then convolved with the WWSSN 15–100 instrument responses and Futterman's attenuation operator with  $t^* = 1$  for  $P$ -waves and  $t^* = 4$  for  $S$ -waves. The source time function was parameterized as a series of boxcars, each of 1 s duration. The synchronization of the initial points of the windowed Green's functions with the associated body wave data was very carefully performed since it plays a critical role in the inversions. The short-period records were primarily used in the cases of nodal stations to identify the  $P$  arrival. In all cases, the waveform data showed a strong interference of phases at the beginning of the records which suggested a shallow source depth, < 15 km.

A different number of boxcar elements was tested, so as to avoid truncating the time function. Inversions for the moment tensor and 8–10 time function elements were performed with the source at 3, 6, 9, 10, 12 and 15 km depth. Five iterations were performed, with rapid convergence within three. In this study, the parameters were not weighted, and Wiggins covariance matrix for the data was assumed to be the identity matrix. During the test inversions a cut-off value for the maximum allowable variance of the parameter changes was arbitrarily set so that all parameters were well resolved and any singular values are assumed to be zero. The waveforms of the  $S$ -waves, registering larger amplitudes than those of the  $P$ -waves, commanded a higher importance in the inversion and were therefore preferentially fit by the synthetics. The  $S$ -wave data were weighted to equalize their importance, with no significant change in the synthetics.

Indicators of the performance of the inversion are the RMS error, measure of the fit of the synthetics to the data, and the least-square's error, LSE, a measure of the overall quality of the inversion. Finally, the compensated linear vector dipole, CLVD, is the remainder following the rotation of the moment tensor into its principal axes and its decomposition into a major double-couple. Plots of the variation of RMS, LSE and CLVD with depth were used to determine an optimum source depth for each case. Minima were revealed for  $d = 10$  km for the event of February 19, 1968, for  $d = 6$  km for December 19, 1981 and for  $d = 9$  km for the

Table 3

*Inversion results*

Inversion Parameters Moment Tensor	Febr 19, 1968		Dec 19, 1981		Aug 6, 1983	
	<i>p</i>	$\sigma \Delta p$	<i>p</i>	$\sigma \Delta p$	<i>p</i>	$\sigma \Delta p$
$M_{11} \times 10^{25}$ dyn.cm	-21.1	0.078	-20.5	0.076	-11.2	0.005
$M_{22} \times 10^{25}$ dyn.cm	+21.01	0.077	+21.1	0.079	+11.9	0.006
$M_{12} \times 10^{25}$ dyn.cm	+6.24	0.071	-0.62	0.086	-1.97	0.005
$M_{13} \times 10^{25}$ dyn.cm	+4.72	0.026	-0.06	0.073	-2.18	0.002
$M_{23} \times 10^{25}$ dyn.cm	-0.13	0.016	-8.06	0.056	-1.91	0.002
$M_0 \times 10^{25}$ dyn.cm	22.42		22.38		12.11	
Time Function	<i>p</i>	$\sigma \Delta p$	<i>p</i>	$\sigma \Delta p$	<i>p</i>	$\sigma \Delta p$
$S_1$	0.102	0.0018	0.074	0.0014	0.152	0.0026
$S_2$	0.095	0.0030	0.061	0.0022	0.065	0.0041
$S_3$	0.168	0.0036	0.147	0.0024	0.188	0.0045
$S_4$	0.155	0.0039	0.154	0.0025	0.208	0.0046
$S_5$	0.149	0.0039	0.130	0.0024	0.151	0.0046
$S_6$	0.163	0.0036	0.158	0.0025	0.132	0.0045
$S_7$	0.066	0.0030	0.093	0.0024	0.082	0.0041
$S_8$	0.102	0.0019	0.085	0.0024	0.022	0.0026
$S_9$			0.065	0.0022		
$S_{10}$			0.032	0.0014		
Principal Axes	<i>AZ</i> °	Plunge°	<i>AZ</i> °	Plunge°	<i>AZ</i> °	Plunge°
Pressure Axis	78	5	270	20	273	7
Intermediate Axis	340	78	90	71	152	75
Tension Axis	170	13	280	0	6	14
RMS FIT ( $\mu\text{m} \times 10^0$ )	8.31		5.56		3.19	
LEAST SQUARE ERROR	0.26 ( $\mu\text{m}^2 \times 10^4$ )		0.20 ( $\mu\text{m}^2 \times 10^4$ )		0.11 ( $\mu\text{m}^2 \times 10^0$ )	
ERROR CLVD	4.62%		14.7%		3.7%	

event of August 6, 1983. Table 3 lists the inversions results for the above-mentioned source depths, i.e., the moment tensor elements, the time-function elements, the standard error of the parameter changes ( $\sigma \Delta p$ ), computed assuming 10% error in the data amplitudes and the major double-couple parameters for each event.

### 2.1. Event of February 19, 1968

Figures 2 and 3 display the inverted *P* and *SH* waveforms and the resulting synthetics for a source depth of 10 km. The nodal surfaces of the moment tensor and its major double-couple are also plotted on a lower hemisphere equal area projection (broken lines on the figures). Both the synthetics and the waveforms are normalized to their maximum amplitude, shown to the right side of each trace (in microns). The synthetics exhibit a good fit in amplitude and overall shape, within the inversion window, though they fail to fit the distortions observed in the waveforms. LANGSTON (1977) notes that teleseismic *P*-waves radiated from sources

FEBRUARY 19, 1968  
P - WAVES

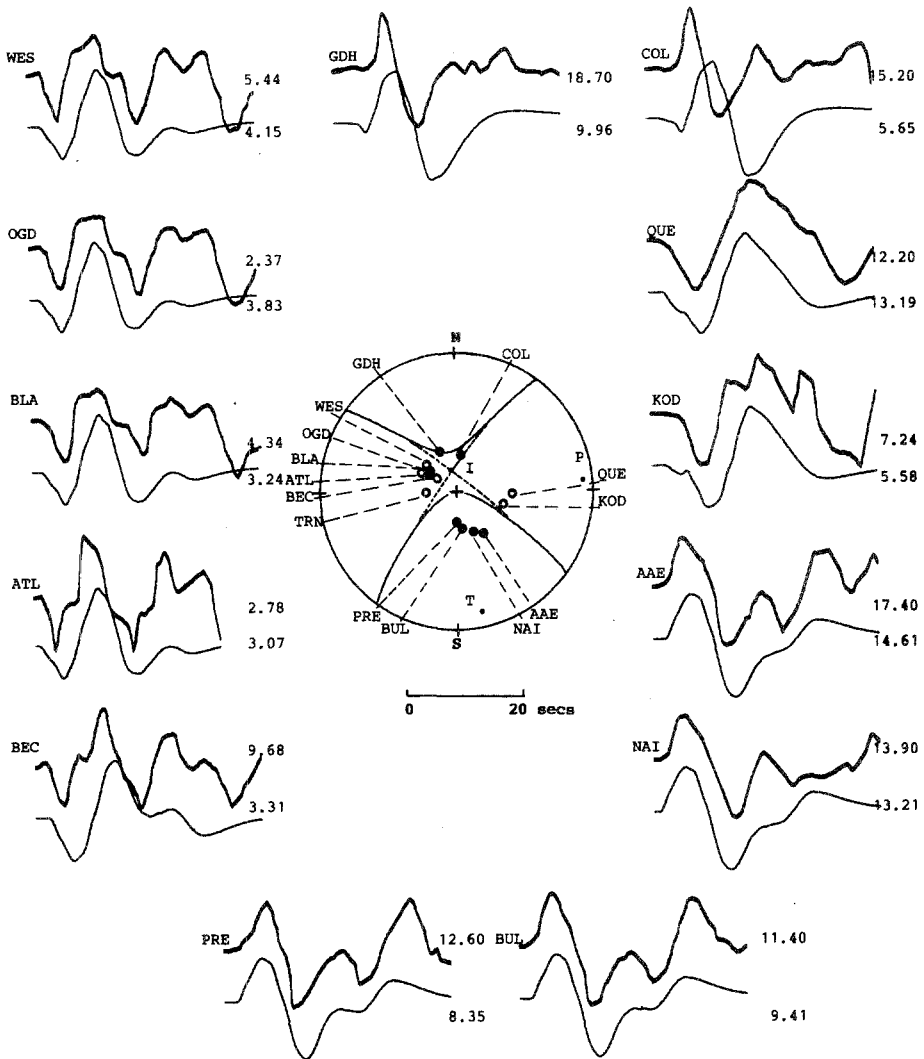


Figure 2

Observed (top) and synthetic (bottom) *P* waveforms for the event of February 19, 1968. The waveforms are normalized to their maximum amplitude, indicated to the right of each trace. The moment tensor nodal surfaces (solid lines) and its major double-couple (dashed lines) are also shown in a lower hemisphere equal area projection. The location and the polarities of *P*-wave first motions are also shown on the figure.

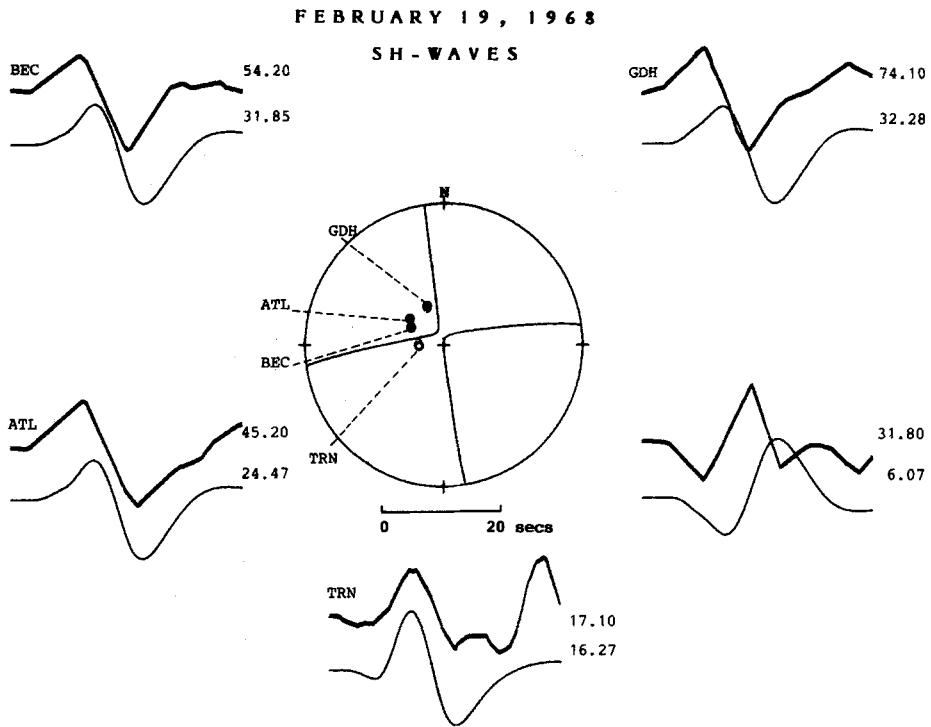


Figure 3

Observed and synthetic *SH* waveforms for the event of February 19, 1968. Notation the same as Figure 2.

whose radiation pattern varies rapidly with azimuth (e.g., strike-slip faults) can be greatly distorted by a dipping structure at the source. It is probable that the misfit observed in the long period *P*-waveforms of the events studied here is attributed to the nonhorizontal nature of the sea floor in the epicentral region, since strike-slip sources show the greatest sensitivity to bathymetric dip (WIENS, 1987).

MCKENZIE (1972) based on first motion data, presents a strike-slip solution for this event with a normal component (strike  $205^\circ$ , dip  $70^\circ$ NW and strike  $114^\circ$ , dip  $87^\circ$ SW). The fault planes obtained here with the moment tensor analysis are in favorable agreement with MCKENZIE's (1972). We favor the NE striking plane as the fault plane because it parallels the general trend of the Anatolian fault.

This earthquake occurred near the island of Agios Efstratios. Field observations and air photograph analysis of the surface fault trace, which cuts the island in a NE-SW trend, and is associated with the 1968 shock, show a dextral strike-slip motion with normal component (PAVLIDES *et al.*, 1989).

The seismic moment, determined by dividing the modulus of the moment tensor by  $\sqrt{2}$ , is  $2.24 \times 10^{26}$  dyn.cm. The average stress drop, assuming a circular crack, is of the order of 13 bars.



## 2.2. Event of December 19, 1981

The epicenter of this earthquake ( $39.1^{\circ}\text{N}$ ,  $25.2^{\circ}\text{E}$ ) was located in the sea west of the island of Lesbos. On December 27, 1981, its largest aftershock of  $M_s = 6.5$  occurred in the southwesternmost part ( $38.8^{\circ}\text{N}$ ,  $24.9^{\circ}\text{E}$ ) of the aftershock area. On January 18, 1982, one month after the first shock, a new seismic sequence started, with an earthquake of  $M_s = 7.0$  and an epicenter ( $39.8^{\circ}\text{N}$ ,  $24.5^{\circ}\text{E}$ ) located 60 km northwest of the epicenter of December 19, 1981 (PAPAZACHOS *et al.*, 1984).

Figures 4 and 5 show the inverted  $P$  and  $SH$  waveforms and the resulting synthetics for a source depth of 6 km. The inversion yielded a dextral strike-slip fault, with strike  $47^{\circ}$ , dip  $77^{\circ}$  (ESE), rake  $193^{\circ}$  for one plane and strike  $314^{\circ}$ , dip  $78^{\circ}$  (WNW) and rake  $-14^{\circ}$  for the other. This mechanism is slightly different from the one proposed by PAPAZACHOS *et al.* (1984), based on first motions of long and short period  $P$ -waves.

The focal mechanism for the largest aftershock of December 27, 1981, determined by KING and KIRATZI (1985) by forward modeling, manifests an almost

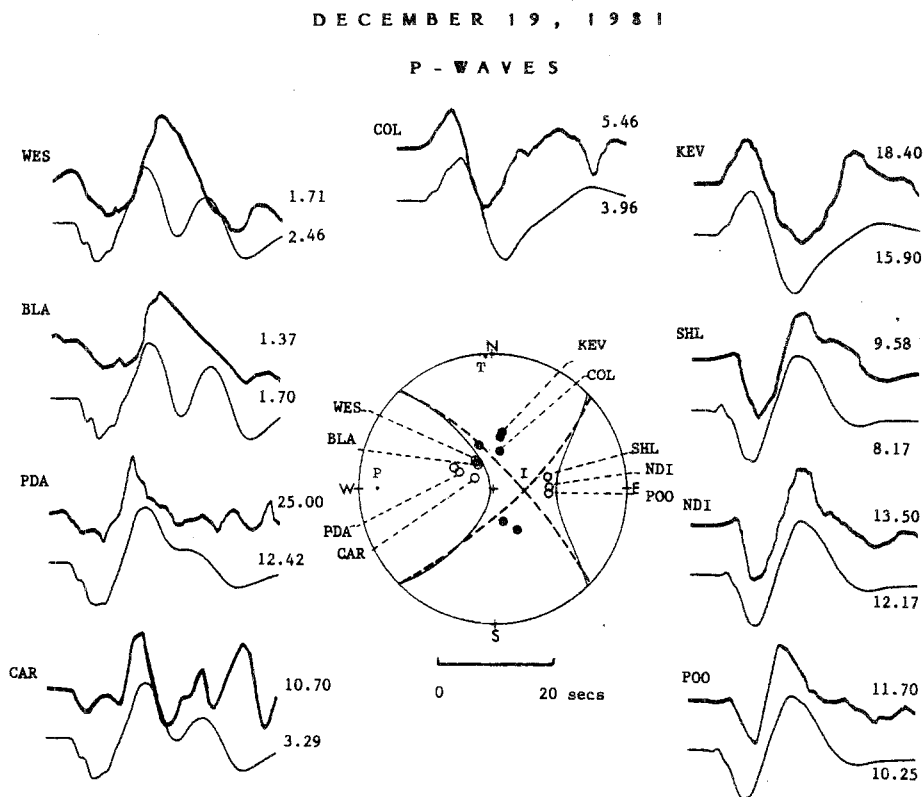


Figure 4  
Same as Figure 2 for the event of December 19, 1981.

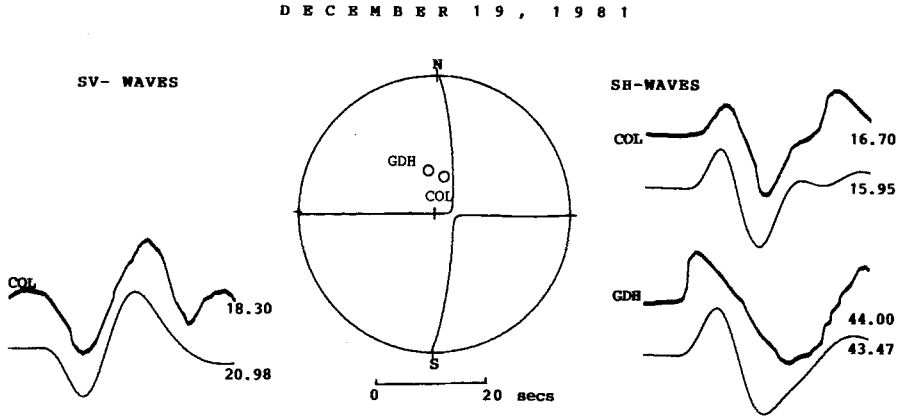


Figure 5

Observed and synthetic *SV* and *SH* waveforms for the event of December 19, 1981. Notation as in Figure 3.

pure strike-slip fault with strike  $33^\circ$ , dip  $87^\circ$  and rake  $188^\circ$ . As for the event of January 18, 1982 an attempt was made to model its source parameters utilizing moment tensor inversion. However, the data were few and noisy and the inversion parameters were not well resolved. Regardless, all the solutions for this event yielded strike-slip faulting with a strong thrust component. PAPAACHOS *et al.* (1984), also using *P* polarities, determine a strike-slip fault with strike  $56^\circ$ , dip  $50^\circ$  (WNW) and rake  $26^\circ$ .

The seismic moment of the event of December 19, 1981, determined by the inversion, is  $2.24 \times 10^{26}$  dyn.cm while the average stress drop, assuming a circular crack with the fault area determined by the aftershocks (KIRATZI *et al.*, 1985), is 8 bars. Using  $M_0$  as it was determined by the inversion and a downdip width equal to twice the focal depth divided by the sine of the dip angle, an average slip of 67.3 cm was obtained ( $\mu = 3 \times 10^{11}$  dyn.cm $^{-2}$ ).

### 2.3. Event of August 6, 1983

This was a widely felt earthquake which occurred 30 km WNW of the island of Limnos ( $40.08^\circ\text{N}$ ,  $24.78^\circ\text{E}$ ). Figures 6 and 7 display the inverted *P*, *SV* and *SH* waveforms and the resulting synthetics for a source depth of 9 km. In this case also, the synthetics show favorable fit in overall shape and amplitude. The focal mechanism corresponds to a dextral strike-slip fault with strike  $50^\circ$ , dip  $76^\circ$ , rake  $177^\circ$ , for one plane and strike  $140^\circ$ , dip  $87^\circ$  and rake  $14^\circ$  for the other. This mechanism corresponds well with the one determined by ROCCA *et al.* (1985), based on first motion data.

The seismic moment determined by the inversion is  $1.21 \times 10^{26}$  dyn.cm while the

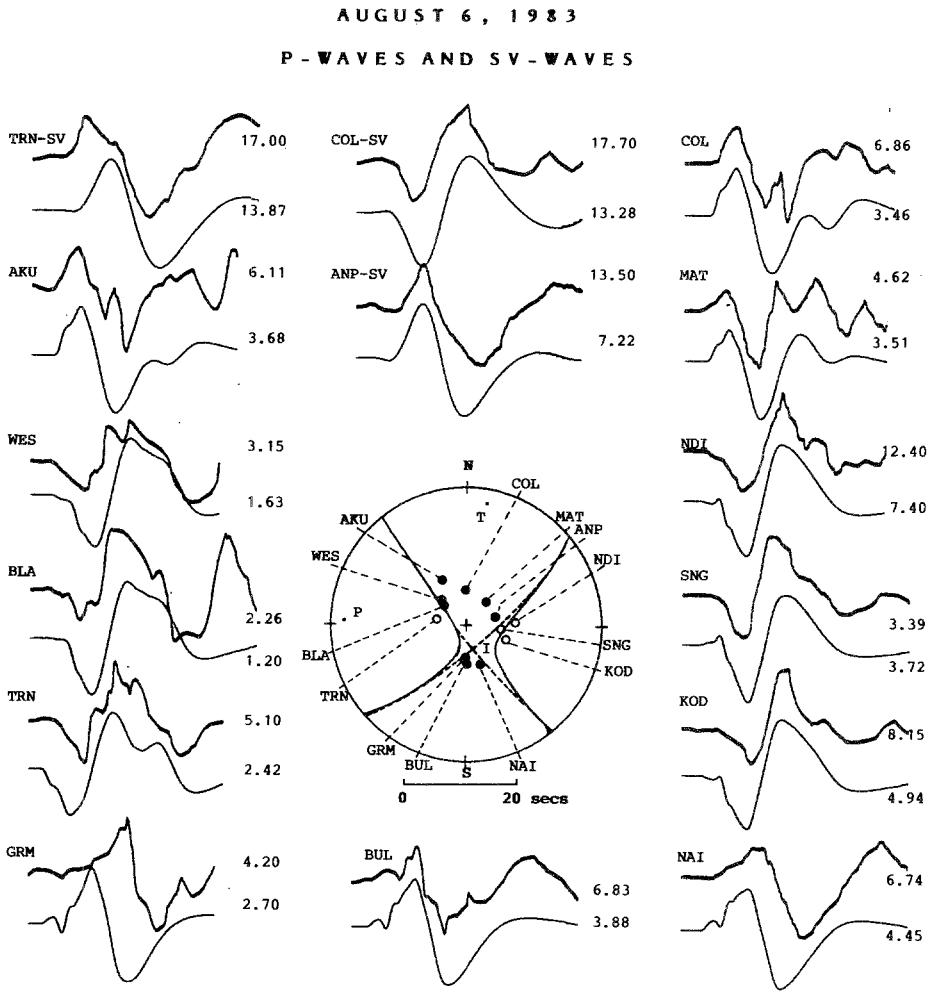


Figure 6

Observed and synthetic *P* and *SV* waveforms for the event of August 6, 1983. Notation as in Figure 2.

average stress drop, assuming a circular crack, is approximately 28 bars. The average slip, calculated as before, was found equal to 45.5 cm.

### 3. Conclusions and Discussion

Source mechanisms, depths, seismic moments and source time functions have been obtained for the events of February 19, 1968, December 19, 1981 and of August 6, 1983 occurring in the Northern Aegean, employing the moment tensor inversion formalism. The observed waveforms of these events exhibited prominent

AUGUST 6, 1983

## SH - WAVES

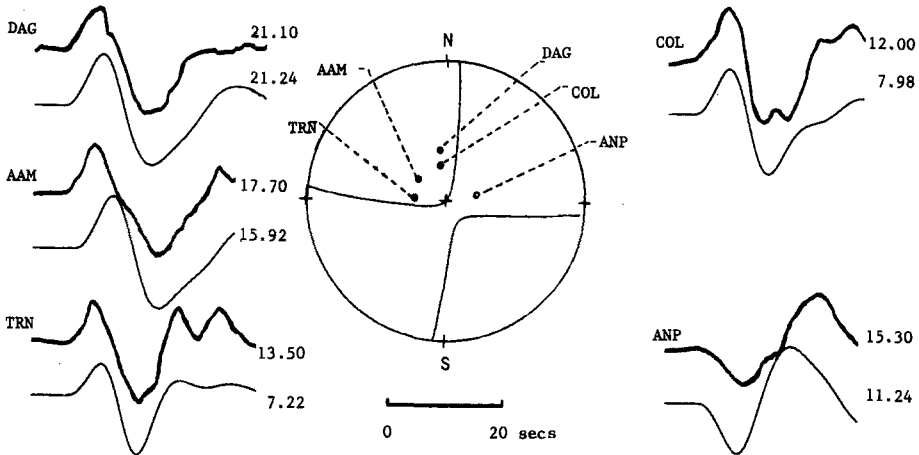


Figure 7

Same as Figure 3 for the event of August 6, 1983.

water multiples and complexity which were not modelled by the moment tensor inversion, assuming a point source and a flat lying bathymetry in the epicentral regions. Examination of the improvement of the synthetics with a structure model containing dipping layers at the source will be the scope of future work.

All focal depths determined are shallow ( $\leq 10$  km) which places the source in the crust and intensifies previous suggestions that the strain rate in the Aegean is high enough to raise the isotherm representing the seismic-aseismic transition above its more typical continental depth of around 15 km (JACKSON and MCKENZIE, 1988).

The derived focal mechanisms of the events studied exhibit dextral strike-slip faulting. As previously stated the Northern Aegean is tectonically controlled by the NS extension the whole Aegean is undergoing and the motion of the westward part of the strike-slip North Anatolian fault. The moment tensor elements and the focal mechanisms of the events studied are in very good agreement with this tectonic regime.

#### Acknowledgements

This work was completed while AAK was visiting Penn State University. The authors would like to thank Prof. Papazachos of the Geophysical Laboratory, of the University of Thessaloniki for his helpful suggestions. This work was supported by a NSF grant EAR85-17626.

## REFERENCES

- BARKER, G. B., and LANGSTON, C. (1982), *Moment Tensor Inversion of Complex Earthquakes*, Geophys. J. R. Astr. Soc. 68, 777–803.
- COMNINAKIS, P., and PAPAACHOS, B. (1986), *A Catalogue of Earthquakes in Greece and the Surrounding Area for the Period 1901–1985*, Publication of the Geophysical Laboratory, University of Thessaloniki, No 1, 1986.
- JACKSON, J., and MCKENZIE, D. (1988), *The Relationship between Plate Motions and Seismic Moment Tensors, and the Rates of Active Deformation in the Mediterranean and Middle East*, Geophys. J. 93, 45–73.
- KARACOSTAS, B., HATZIDIMITRIOU, P., KARAKAISIS, G., PAPANIMITRIOU, E., and PAPAACHOS, B. (1986), *Evidence for Long-term Precursors of Strong Earthquakes in the Northernmost Part of the Aegean Sea*, Earthquake Pred. Res. 4, 155–164.
- KING, G., and KIRATZI, A. (1985), *Forward Modelling of the December 27, 1981 North Aegean Event* (unpublished data).
- KIRATZI, A., KARAKAISIS, G., PAPANIMITRIOU, E., and PAPAACHOS, B. (1985), *Seismic-source Parameter Relations for Earthquakes in Greece*, Pure Appl. Geophys. 123, 27–41.
- LANGSTON, C. A. (1977), *The Effect of Planar Dipping Structure on Source and Receiver Responses for Constant Ray Parameter*, Bull. Seismol. Soc. Am. 67, 1029–1050.
- LANGSTON, C. A. (1981), *Source Inversion of Seismic Waveforms: The Koyna, India, Earthquakes of 13 September 1967*, Bull. Seismol. Soc. Am. 71, 1–24.
- LANGSTON, C., and HELMBERGER, D. (1975), *A Procedure for Modelling Shallow Dislocation Sources*, Geophys. J. R. Astr. Soc. 42, 117–130.
- LEPICHON, X., and ANGELIER, J. (1979), *The Hellenic Arc and Trench System: A Key to the Neotectonic Evolution of the Eastern Mediterranean Area*, Tectonophysics 60, 1–42.
- MCKENZIE, D. (1972), *Active Tectonics of the Mediterranean Region*, Geophys. J. R. Astr. Soc. 30, 109–185.
- MCKENZIE, D. (1978), *Active Tectonics of the Alpine-Himalayan Belt: The Aegean Sea and Surrounding Regions*, Geophys. J. R. Astr. Soc. 55, 217–254.
- PANAGIOTOPOULOS, D., and PAPAACHOS, B. (1985), *Travel Times of Pn Waves within the Aegean and Surrounding Area*, Geophys. J. R. Astr. Soc. 80, 165–176.
- PAPAACHOS, B., KIRATZI, A., VOIDOMATIS, Ph., and PAPAIOANNOU, C. (1984), *A Study of the December 1981–January 1982 Seismic Activity in Northern Aegean Sea*, Boll. di Geof. Teor. ed Appl. XXVI, 101–102, 101–113.
- PAPAACHOS, B., KIRATZI, A., HATZIDIMITRIOU, P., and KARACOSTAS, B. (1986), *Seismotectonic Properties of the Aegean Area that Restrict Valid Geodynamic Models*, Wegener/Medias Conference, Athens, May 14–16, 1986, 1–20.
- PAVLIDES, S., MOUNTRAKIS, D., KILIAS, A., and TRANOS, M. (1989), *The role of strike-slip movements in the extensional area of Northern Aegean (Greece)*, Workshop on Active and Recent Strike-slip Tectonics, Florence Univ., 18–20 April 1989 (Abstr.).
- PAVLIN, G., and LANGSTON, C. A. (1983), *The Inverse Problem: Implications of Surface Waves and Free Oscillations for Earth Structure*, Rev. Geophys. Space Phys. 10, 251–282.
- ROCCA, A., KARAKAISIS, G., KARACOSTAS, B., KIRATZI, A., SCORDILIS, E., and PAPAACHOS, B. (1985), *Further Evidence on the Strike-slip Faulting of the Northern Aegean Trough Based on Properties of the August–November 1983 Seismic Sequence*, Boll. di Geof. Teor. ed Appl. XXVII, 106, 101–109.
- WIENS, D. (1987), *Effects of Near-source Bathymetry on Teleseismic P Waveforms*, Geophys. Res. Lett. (in press).

(Received April 16, 1990, accepted November 30, 1990)